Development 135, 755-765 (2008) doi:10.1242/dev.012708

Recombinase-mediated cassette exchange reveals the selective use of G_q/G_{11}-dependent and -independent endothelin 1/endothelin type A receptor signaling in pharyngeal arch development

Takahiro Sato[1,2], Yumiko Kawamura[1], Rieko Asai[1], Tomokazu Amano[3], Yasunobu Uchijima[1], Dagmara A. Dettlaff-Swiercz[4], Stefan Offermanns[4], Yukiko Kurihara[1] and Hiroki Kurihara[1,*]

The endothelin (Edn) system comprises three ligands (Edn1, Edn2 and Edn3) and their G-protein-coupled type A (Ednra) and type B (Ednrb) receptors. During embryogenesis, the Edn1/Ednra signaling is thought to regulate the dorsoventral axis patterning of pharyngeal arches via *Dlx5*/*Dlx6* upregulation. To further clarify the underlying mechanism, we have established mice in which gene cassettes can be efficiently knocked-in into the *Ednra* locus using recombinase-mediated cassette exchange (RMCE) based on the Cre-lox system. The first homologous recombination introducing mutant *lox*-flanked *Neo* resulted in homeotic transformation of the lower jaw to an upper jaw, as expected. Subsequent RMCE-mediated knock-in of *lacZ* targeted its expression to the cranial/cardiac neural crest derivatives as well as in mesoderm-derived head mesenchyme. Knock-in of *Ednra* cDNA resulted in a complete rescue of craniofacial defects of *Ednra*-null mutants. By contrast, *Ednrb* cDNA could not rescue them except for the most distal pharyngeal structures. At early stages, the expression of *Dlx5*, *Dlx6* and their downstream genes was downregulated and apoptotic cells distributed distally in the mandible of *Ednrb*-knock-in embryos. These results, together with similarity in craniofacial defects between *Ednrb*-knock-in mice and neural-crest-specific $G\alpha_q/G\alpha_{11}$-deficient mice, indicate that the dorsoventral axis patterning of pharyngeal arches is regulated by the Ednra-selective, G_q/G_{11}-dependent signaling, while the formation of the distal pharyngeal region is under the control of a G_q/G_{11}-independent signaling, which can be substituted by Ednrb. This RMCE-mediated knock-in system can serve as a useful tool for studies on gene functions in craniofacial development.

KEY WORDS: Endothelin, G protein-coupled receptor, Pharyngeal arch, Neural Crest, Mouse

INTRODUCTION

Craniofacial development in vertebrates is a complex process involving the coordinated interaction of different cell populations. During neural tube formation, cranial neural crest cells originate at the border between the neural plate and the surface ectoderm, and migrate ventrolaterally to contribute to the head mesenchyme together with mesodermal cells (Chai and Maxson, Jr, 2006; Le Douarin and Kalcheim, 1999; Noden and Trainor, 2005). The pharyngeal arches, the segmental structures of the embryonic head covered by ectoderm- and endoderm-derived epithelium, are populated with neural crest cells from the hindbrain and caudal midbrain, where they surround a mesodermal core. Within each pharyngeal arch, complex cellular interactions are thought to determine their regional identity and cell fates (Le Douarin and Kalcheim, 1999; Noden and Trainor, 2005).

In the two anterior pharyngeal arches, the first and second arches, dorsoventral axis patterning predominates the appropriate formation of chondrocranial elements and associated dermal bones (Kontges and Lumsden, 1996; Le Douarin and Kalcheim, 1999). The first pharyngeal arch is subdivided along the dorsoventral axis into the maxillary and mandibular arches, which give rise to the upper and lower jaws, respectively. Recently, molecules involved in the determination of their identities have been explored and the *Dlx* genes, vertebrate *Distal-less* homologs, have been thought to play a key role (Depew et al., 2005; Merlo et al., 2000). Among the six known *Dlx* genes, *Dlx5* and *Dlx6* are expressed in the ventral part within the anterior pharyngeal arches (Depew et al., 2005; Merlo et al., 2000). *Dlx5*/*Dlx6* double null-mutant mice demonstrate homeotic transformation of the lower jaw into an upper jaw, indicating that *Dlx5* and *Dlx6* are major determinants of the mandibular identity (Beverdam et al., 2002; Depew et al., 2002).

The endothelin (Edn) system, composed of three peptide ligands (Edn1, Edn2 and Edn3) and their two G-protein-coupled receptors [endothelin type A receptor (Ednra) and type B receptor (Ednrb)], is involved in diverse biological events (Kedzierski and Yanagisawa, 2001; Kurihara et al., 1999; Masaki, 2004). These receptors activate an overlapping set of G proteins (e.g. G_q/G_{11}), leading to various intracellular responses such as activation of phospholipase C, increase in intracellular calcium and induction of early responsive genes (Kedzierski and Yanagisawa, 2001). During embryogenesis, the Edn1-Ednra axis regulates craniofacial and cardiovascular morphogenesis, whereas the Edn3-Ednrb axis contributes to melanocyte and enteric neuron development (Kedzierski and Yanagisawa, 2001; Kurihara et al., 1999; Masaki, 2004).

In craniofacial development, *Edn1* is expressed in the epithelium and mesodermal core of the pharyngeal arches, whereas *Ednra* is in neural crest-derived ectomesenchyme (Clouthier et al., 1998; Kurihara et al., 1995; Kurihara et al., 1994; Maemura et al., 1996). Defects in the Edn1/Ednra pathway results in the malformation of pharyngeal-arch-derived craniofacial

[1]Department of Physiological Chemistry and Metabolism, Graduate School of Medicine, The University of Tokyo, 7-3-1 Hongo, Bunkyo-ku, Tokyo 113-0033, Japan. [2]Tsukuba Safety Assessment Laboratories, Banyu Pharmaceutical Company Limited, 3 Okubo, Tsukuba, Ibaraki 300-2611, Japan. [3]Department of Developmental Medical Technology (Sankyo), Graduate School of Medicine, The University of Tokyo, 7-3-1 Hongo, Bunkyo-ku, Tokyo 113-0033, Japan. [4]Institute of Pharmacology, University of Heidelberg, Im Neuenheimer Feld 366, 69120, Heidelberg, Germany.

*Author for correspondence (e-mail: kuri-tky@umin.ac.jp)

Accepted 15 November 2007

structures in mice (Clouthier et al., 1998; Kurihara et al., 1995; Kurihara et al., 1994), rats (Spence et al., 1999), birds (Kempf et al., 1998) and fish (Kimmel et al., 2003; Miller et al., 2000). Homeotic transformation of the mandibular arch with downregulation of *Dlx5*/*Dlx6* in *Edn1*-null embryos implicates the Edn1/Ednra pathway in the dorsoventral axis patterning of the pharyngeal arch system as a positive regulator of *Dlx5*/*Dlx6* expression (Kurihara et al., 1994; Ozeki et al., 2004; Ruest et al., 2004). Although the G_q/G_{11}-mediated signaling pathway has been suggested to be involved in pharyngeal arch development (Dettlaff-Swiercz et al., 2005; Ivey et al., 2003; Offermanns et al., 1998), the intracellular signaling pathway coupling the Edn1-Ednra system to the induction of *Dlx5*/*Dlx6* remains unknown.

To investigate the intracellular signaling mechanism involving the Edn1/Ednra pathway in craniofacial development, we choose a knock-in strategy with a recombinase-mediated cassette exchange (RMCE) using the Cre-*lox* system. This method enables an efficient exchange of a chromosomal region flanked by incompatible mutant *lox* sequences for a cassette located on a plasmid, and is highly advantageous in that it allows the repetitive use of the same embryonic stem (ES) cell line to insert various genes of interest into the identical recombinant allele (Sorrell and Kolb, 2005). Here we have established an *Ednra* knock-in system using RMCE. Knock-in of the *lacZ* gene resulted in the visualization of *Ednra*-expressing cells. Furthermore, knock-in of *Ednra* and *Ednrb* revealed Ednra-selective and non-selective signaling pathways operating in distinct regions. *Ednrb* knock-in mice, which demonstrated homeotic transformation of the lower jaw into an upper jaw but had relatively well-developed incisive alveolar bone and hyoid, resembled neural-crest-specific $G\alpha_q/G\alpha_{11}$-deficient mice. Together with differences in distal pharyngeal-arch-derived structures between these mice and Ednra-null mice, these results indicate that G_q/G_{11}-dependent and -independent Edn1/Ednra pathways, which may correspond to Ednra-selective and non-selective signaling, respectively, are used in different contexts during pharyngeal arch development.

MATERIALS AND METHODS

Plasmid construction

A C57BL6-derived BAC clone containing the mouse *Ednra* gene was obtained from BACPAC Resource Center (Oakland). The targeting construct was designed to replace a 1.0 kb sequence containing the ATG translation start site in exon2 with the *PGK*-neomycin resistance gene cassette (*Neo*) flanked with *lox71* at the 5′ end and *lox2272* with the bovine growth hormone polyadenylation signal at the 3′ end (see Fig. 1). A PCR-amplified 1.1 kb fragment encompassing intron1 to exon2 and a 9.2 kb *Cla*I-*Bam*HI fragment from intron 2 were placed on each side of the floxed *Neo* in a pKO Scrambler NTKV-1904 vector (Stratagene). The *MC1-thymidine kinase* cassette (*TK*) was placed 3′ downstream to the 9.2 kb fragment for negative selection.

The RMCE-mediated knock-in vector was made in a p66-2272 plasmid (Araki et al., 2002). The *PGK*-puromycin resistance gene cassette (*Puro*) was flanked by Flp recombinase target (*FRT*) sequences (Schlake and Bode, 1994) and placed between *lox66* and *lox2272* with multiple cloning sites. For the knock-in of *lacZ*, the *lacZ* gene with an SV40 large T antigen-derived nuclear localization signal was introduced into the multicloning site placed between *lox66* and the *FRT*-flanked *Puro* using appropriate restriction enzymes. For the knock-in of *Ednra* and *Ednrb*, PCR-amplified fragments encoding the open reading frame of mouse *Ednra* and *Ednrb* cDNA were introduced into the knock-in vector in the same way.

Homologous recombination and RMCE in ES cells

The targeting vector was linearized and electroporated into B6129F1-derived ES cell line ATOM1 (Amano et al., unpublished). Clones surviving positive-negative selection with neomycin and FIAU were screened for homologous recombination with genomic PCR using diagnostic primers. Correct recombination was confirmed by Southern blotting using the probes indicated in Fig. 1. For RMCE, the ES cell line in which the initial recombination was successfully achieved was used repeatedly. ES cells were infected with AxCANCre, recombinant adenovirus expressing the recombinase Cre tagged with a nuclear localization signal under the control of the CAG promoter (Kanegae et al., 1995). Forty-eight hours later, ES cells were electroporated with the knock-in vector and seeded onto multidrug-resistant embryonic fibroblasts derived from the DR4 mouse strain (Tucker et al., 1997). Clones selected with 1 μg/ml puromycin were picked up and genotyped by PCR to identify RMCE-mediated recombination.

Mutant mice

Targeted ES clones were injected into ICR blastocysts to generate germline chimeras. For excision of the FRT-flanked *Puro*, the Flp recombinase-expression plasmid pCAGGS-FLPe (Gene Bridges, Dresden, Germany) was injected into the male pronuclei of fertilized eggs having the knocked-in allele. Sequential recombination events were verified by PCR with specific primers, the sequences of which are available on request. Mutant mice were intercrossed with ICR mice and F2 to F5 offspring were subjected to analysis. *P0-Cre*$^{-/+}$;*G*$\alpha_q^{flox/flox}$;*G*$\alpha_{11}^{-/-}$ mice were described previously (Dettlaff-Swiercz et al., 2005). All the animal experiments were performed in accordance with the guidelines of the University of Tokyo Animal Care and Use Committee.

RT-PCR

Expression of knocked-in genes was confirmed by RT-PCR. Primers p (5′-CTGATCCACCGGACCATCGCTGGA-3′) and q (5′-TACCGTTCG-TATAATGTATGCTATACGAACGGTA-3′) were designed to detect transcripts from both *Ednra* and *Ednrb* knocked-in alleles as a 284 bp band. The combination of primers p and r (5′-TCAATGACCAC-GTAGATAAGGT-3′) was designed to detect both endogenous and knocked-in *Ednra* transcripts as 753- and 659 bp bands, respectively. Primer s (5′-GAGAAGTGACAGCGTGGCTT-3′), with primer p, was designed to detect specifically knocked-in *Ednrb* transcripts as a 477 bp product. The housekeeping gene *GAPDH* served as internal control.

Skeletal staining

Alizarin Red/Alcian Blue staining was performed, as previously described (McLeod, 1980).

β-Galactosidase staining

lacZ expression was detected by staining with X-gal (5-bromo-4-chloro-3-indoyl β-D-galactoside) for β-galactosidase activity. Whole-mount staining was performed as previously described (Nagy et al., 2003) with minor modifications. For sections, samples were embedded in OCT compound, cryosectioned and subjected to X-gal staining. Some sections were counterstained with 1% Orange G (Sigma).

In situ hybridization

Whole-mount in situ hybridization was performed as described previously (Wilkinson, 1992). Probes for *Hand2* (Srivastava et al., 1995) and goosecoid (Yamada et al., 1995) were generously provided by D. Srivastava (University of California, San Francisco, CA) and G. Yamada (Kumamoto University, Kumamoto, Japan), respectively. Other probes were prepared by RT-PCR as described (Ozeki et al., 2004).

Apoptosis analysis

For detection of apoptotic cells, terminal deoxynucleotidyl transferase-mediated dUTP nick end labeling (TUNEL) staining was performed on 14 μm consecutive frozen sections of embryonic day 10.5 (E10.5) embryos using a DeadEnd Labeling kit (Promega) with diaminobenzidine as substrate, as previously described (Abe et al., 2007).

RESULTS

Generation of *Ednra-lacZ* knock-in mice by RMCE

We first introduced an exchangeable floxed site into the *Ednra* locus in ES cells to generate the *Ednra*^{neo} allele, which could serve as a target for RMCE (Fig. 1). Electroporation of 1×10^7 ES cells with

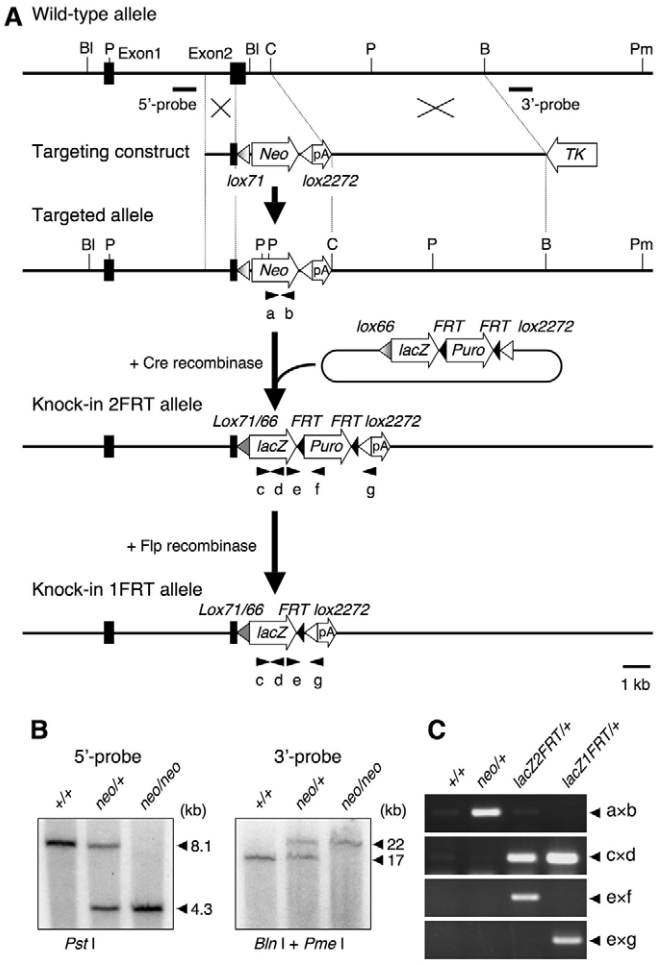

Fig. 1. RMCE in the mouse *Ednra* gene. (**A**) Strategy for targeting and knock-in of *lacZ*. Probes for genotyping are indicated as 5′- and 3′-probes. B, *Bam*HI; Bl, *Bln*I; C, *Cla*I; P, *Pst*I; Pm, *Pme*I. (**B**) Southern blot analysis of *Pst*I- or *Bln*I/*Pme*I-digested genomic DNA of the offspring from an intercross of heterozygotes, probed with the 5′- or 3′-probes, respectively. (**C**) Genomic PCR analysis for sequential Cre-*lox*-mediated recombination with primers indicated in A.

the targeting vector followed by positive-negative selection yielded 224 clones surviving selection, among which 13 clones proved to be correctly recombined and five clones were transmitted through the germline.

One recombinant ES clone capable of efficient germline transmission was used repeatedly for subsequent RMCE. In the present scheme, the expression of a knocked-in gene was expected to recapitulate the endogenous *Ednra* expression patterns. To confirm this and to evaluate the efficiency of RMCE, we introduced the *lacZ* gene into the *Ednra* locus ($Ednra^{lacZ2FRT}$). After infection of AxCANCre and electroporation of *nls-lacZ*-containing knock-in vector, positive selection with puromycin yielded 94 surviving clones, among which 82 clones (87%) were correctly introduced with *lacZ*. Three *lacZ*-carrying clones were transmitted to the germline. Subsequently, we microinjected pCAGGS-FLPe into fertilized eggs obtained from ICR females crossed with $Ednra^{lacZ2FRT/+}$ males to obtain $Ednra^{lacZ1FRT/+}$ mice in which the FRT-flanked *Puro* was removed. All the heterozygotes were viable and fertile.

lacZ-labeling of *Ednra*-expressing cells during embryonic development

To analyze the expression patterns of *Ednra* during postimplantation development, we performed β-galactosidase staining on *Ednra-lacZ* knock-in embryos. *lacZ* expression patterns were identical between $Ednra^{lacZ2FRT/+}$ and $Ednra^{lacZ1FRT/+}$ embryos, indicating that the presence of *Puro* in the mutant allele did not significantly affect the expression of knocked-in genes. Thereafter, pictures of $Ednra^{lacZ2FRT/+}$ embryos stained for β-galactosidase activity are shown.

At E8.25 to 8.5, *lacZ* expression was observed in the head mesenchyme at the hindbrain level (Fig. 2A-C). High magnification of transverse sections at E8.5 revealed *lacZ* expression in migratory neural crest cells delaminating from the dorsal neuroepithelium (Fig. 2D). By contrast, *lacZ* expression was undetectable in the neuroepithelium, including the premigratory neural crest, surface ectoderm, foregut endoderm and vascular endothelium (Fig. 2C,D). At E9.0, *lacZ* was highly expressed in the head and pharyngeal arch regions, in the heart, and in the ventral half of the trunk (Fig. 2E). In the first to third arches, *lacZ* expression was detected in neural-crest-derived ectomesenchymal cells, whereas the pharyngeal ectoderm and endoderm, vascular endothelium and many cells in the core mesenchyme were lacking *lacZ* expression (Fig. 2F). *lacZ* expression was also extensively observed in the head mesenchyme adjacent to the neuroepithelium (Fig. 2F). In the cardiac outflow region, cardiac neural crest cells surrounding the second and third pharyngeal arch arteries and colonizing between the foregut and the aortic sac showed intense *lacZ* expression (Fig. 2G). These *lacZ* expression patterns appeared to recapitulate endogenous *Ednra* expression revealed by in situ hybridization in whole mounts (Fig. 2H) and in sections (Clouthier et al., 1998; Yanagisawa et al., 1998).

By comparison, in situ hybridization of E9.0 embryos for *Crabp1*, a neural crest marker (Ruberte et al., 1992), revealed its expression in the streams of migratory neural crest cells, which overlapped with *Ednra-lacZ* expression (Fig. 2I,L). However, *Ednra-lacZ* expression was also found in *Crabp1*-negative mesenchymal regions ventromedial to the neural crest streams (Fig. 2K). The expression pattern of *Snail1*, which is expressed in neural-crest- and mesoderm-derived head mesenchyme before E10.5 (Nieto et al., 1992; Smith et al., 1992), is more similar to that of *Ednra-lacZ* (Fig. 2J,M). These results suggest that *lacZ*-expressing mesenchymal cells are likely to originate from both neural crest and mesoderm.

At E10.0, *lacZ* expression was observed throughout the head mesenchyme adjacent to the neural tube (Fig. 3A,B). Trigeminal ganglia, which originate in neural crest cells and placode cells, were highly populated with *lacZ*-positive cells (Fig. 3B). In the pharyngeal arches, *lacZ* expression was mainly located in ectomesenchyme underlying the epithelium (Fig. 3A). The distribution of *lacZ* expression within the wall of the aortic sac and pharyngeal arch arteries corresponded to cardiac neural crest cell population (Fig. 3C). At E12.5, *lacZ* expression was found in ectomesenchyme underlying the oral epithelium in the lower and upper jaws (Fig. 3D,G). In developing tooth buds, *lacZ* expression was present in mesenchyme surrounding the endoderm-derived dental lamina (Fig. 3E). In the precartilage primordium of Meckel's cartilage, *lacZ* expression was undetectable in the bilateral rod portion (Fig. 3F), but was intensely present in the rostral process (Fig. 3G,H).

Craniofacial defects of *Ednra*-null mice

As expected, $Ednra^{neo/neo}$, $Ednra^{lacZ/lacZ}$ and $Ednra^{neo/lacZ}$ mice demonstrated perinatal lethality and craniofacial abnormalities, which were almost identical to the phenotype of mice lacking *Edn1*

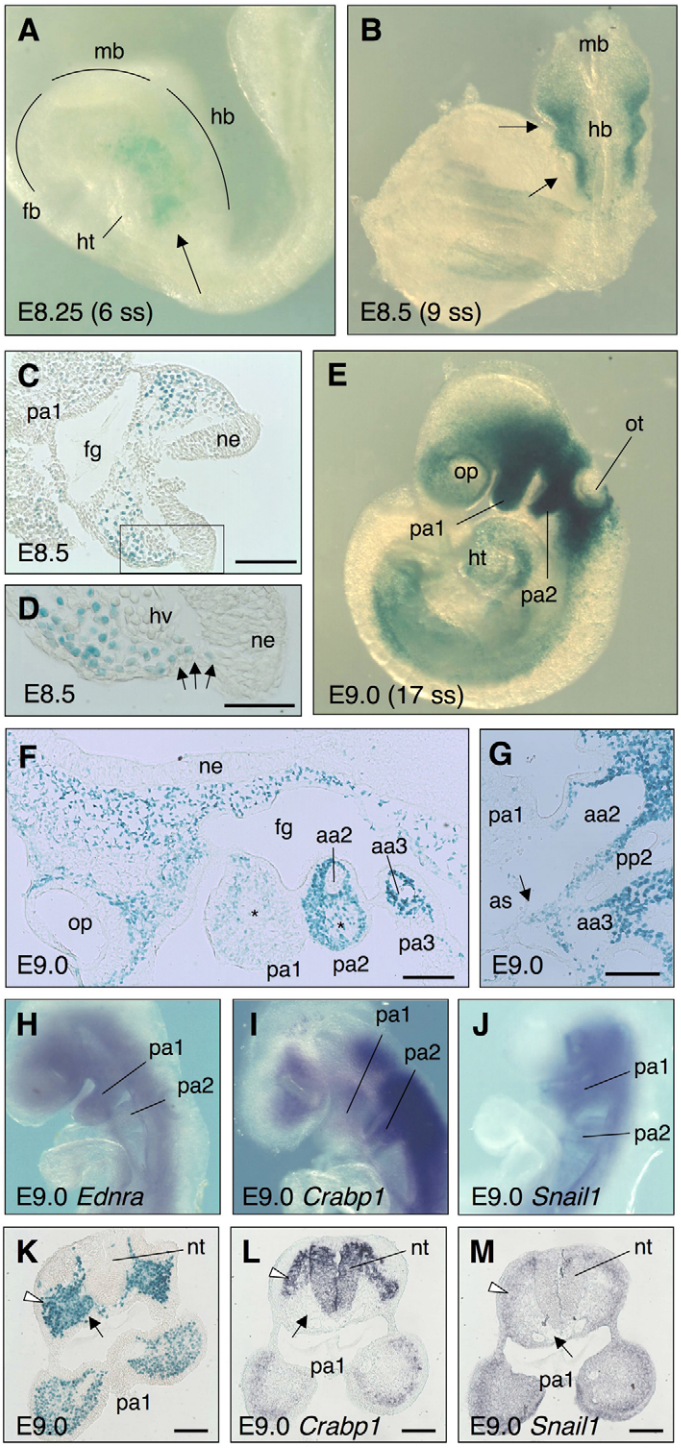

Fig. 2. RMCE-mediated knock-in of *lacZ* into the *Ednra* locus. (**A**,**B**) Whole-mount staining of E8.25 (six-somite stage) (A) and E8.5 (nine-somite stage) (B) *Ednra*$^{lacZ2FRT/+}$ mouse embryos shows *lacZ* expression in the head mesenchyme at the hindbrain level (arrows). (**C**) An E8.5 transverse section at the rostral hindbrain level shows *lacZ* expression in mesenchyme throughout the head and pharyngeal arch regions, but not in the neuroepithelium, surface ectoderm and foregut endoderm. (**D**) High magnification of the boxed area in C demonstrates *lacZ* expression in migratory neural crest cells delaminating from the dorsal neuroepithelium (arrows). (**E**) At E9.0 (17-somite stage), *lacZ* is expressed in the head and pharyngeal arch regions, in the heart, and in the ventral half of the trunk. (**F**) An E9.0 sagittal section in the pharyngeal region demonstrates *lacZ* expression in neural crest-derived ectomesenchyme and in the head mesenchyme adjacent to the neuroepithelium, but not in the pharyngeal epithelium, vascular endothelium and many cells in the core mesenchyme (asterisks). (**G**) The E9.0 cardiac outflow region demonstrates *lacZ* expression in cardiac neural crest cells surrounding the second and third arch arteries and colonizing between the foregut and the aortic sac (arrow). (**H-J**) Whole-mount in situ hybridization of E9.0 wild-type embryos using *Ednra* (H), *Crabp1* (I) and *Snail1* (J) probes. (**K-M**) Comparison between *Ednra-lacZ* expression (K) and in situ hybridization patterns of *Crabp1* (L) and *Snail1* (M) in E9.0 transverse sections at the first pharyngeal arch level. White arrowheads, migratory neural crest cells; arrows, mesoderm-derived mesenchyme. Scale bars: 100 μm in C,F,G,K-M; 50 μm in D. aa2/3, second and third arch arteries; as, aortic sac; fb, forebrain; fg, foregut; hb, hindbrain; ht, heart; hv, head vein; mb, midbrain; ne, neuroepithelium; nt, neural tube; op, optic vesicle; ot, otic vesicle; pa1/2/3, first, second and third pharyngeal arches; pp2, second pharyngeal pouch.

or *Ednra* (Ozeki et al., 2004; Ruest et al., 2004). In these mutants, the lower jaw appeared as a mirror image of the upper jaw with arrays of vibrissae (Fig. 4A,B). Skeletal analysis revealed transformation of mandibular arch-derived structures into maxillary arch-derived elements in mutants (Fig. 4C-F). Most of the dentary was replaced with an ectopic bone, which appeared as a mirror image duplication of the ipsilateral maxilla (Fig. 4G,H), the morphology of which was almost identical to that of wild-type maxillae (Fig. 4I). In addition, a second set of jugal and palatine bones was observed in mutants (Fig. 4E,F). In the most distal portion, alveolar bone was formed around a tiny rostral process of Meckel's cartilage and surrounded a lower incisor, although its growth was variable among individuals (Fig. 4F,G). Zygomatic processes of the squamosal were malformed and often absent (Fig. 4F). In addition, ectotympanic and gonial bones were lost, whereas the pterygoid process, ala temporalis and lamina obturans were duplicated in mutants (Fig. 4J,K). The malleus and incus were malformed, giving an ectopic structure extending to the squamosal (Fig. 4L,M).

Among the second-arch-derived structures, the mutant hyoid was aberrantly ossified and fused bilaterally to the basisphenoid in *Ednra*-null mutants (Fig. 4N,O). The stapes in mutants retained its normal appearance, but was displaced out of the fenestra ovalis and was connected to the hyoid through a cartilaginous strut (Fig. 4L,M). This strut was likely to be a transformed lesser horn of the hyoid, which was fused to the hyoid body and stretched to the lateral side. In addition, the styloid process was truncated in mutants (Fig. 4L,M).

Knock-in of *Ednra* cDNA rescued the *Ednra*-null phenotype

Recapitulation of *Ednra* expression by the RMCE-mediated knock-in of *lacZ* may justify the application of this system for the functional analysis of the Edn1/Ednra signaling mechanism in embryonic development. To confirm this, we introduced *Ednra* cDNA into the *Ednra*^{neo} allele, expecting rescue of the *Ednra*-null phenotype by restoring *Ednra* expression (Fig. 5A). The efficiency of RMCE-mediated knock-in in ES cells was 44% (41 in 94 surviving clones). Four clones generated germline chimeras

following blastocyst injection. Chimeric and heterozygous mice carrying the *Ednra* knock-in allele (*Ednra*^{A}) were intercrossed with *Ednra*$^{lacZ/+}$ mice to obtain *Ednra*$^{lacZ/A}$ offspring.

Mice with the genotype *Ednra*$^{lacZ/A}$ were viable and fertile. Their appearance (Fig. 5B) and craniofacial skeletal morphology (Fig. 5D) were indistinguishable from those of wild-type and *Ednra*$^{lacZ/+}$ heterozygous mice (Fig. 4A,C). These results indicate that the knocked-in *Ednra* cDNA can restore the function of endogenous *Ednra* at least in craniofacial development, which validates the usefulness of the present RMCE-mediated knock-in system for functional analysis.

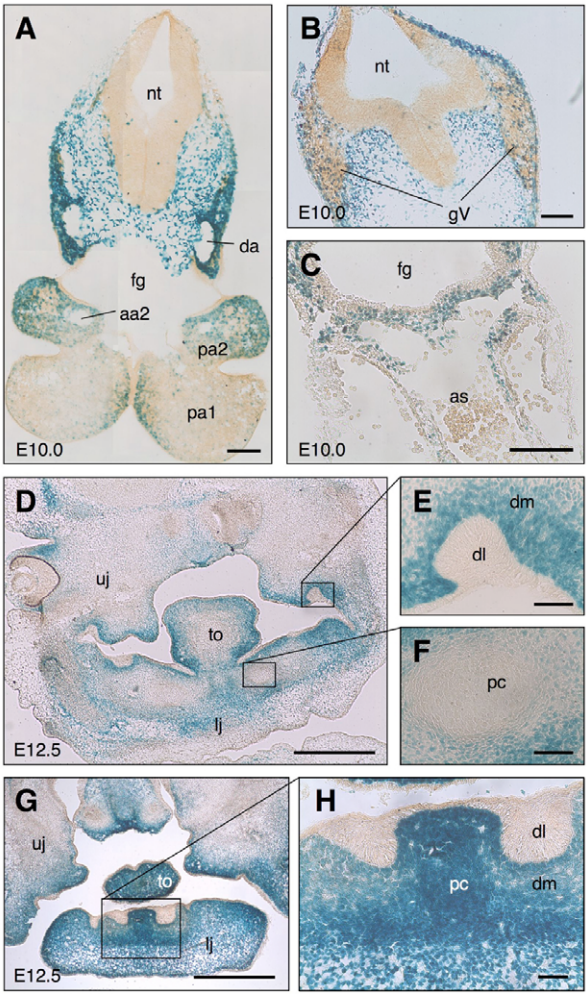

Fig. 3. *LacZ* expression in the head mesenchyme and neural-crest derivatives in *Ednra*$^{lacZ2FRT/+}$ mouse embryos. (**A-C**) Transverse sections at E10.0. *LacZ* expression is observed throughout the head mesenchyme adjacent to the neural tube and in the peripheral pharyngeal arch mesenchyme (A). Trigeminal ganglia are highly populated with *lacZ*-positive cells (B). *LacZ* expression is detectable within the lateral wall of the aortic sac and pharyngeal arch arteries (C). (**D-H**) Transverse sections at the levels of the central (D-F) and distal (G,H) regions of the lower jaw at E12.5. E,F,H are high magnification images of the boxed areas in D and G. *LacZ* expression is observed in mesenchyme underlying the oral epithelium in the lower and upper jaws (D,G). In the molar (E) and incisor (H) buds, *lacZ* expression is present in mesenchyme surrounding the dental lamina. *LacZ* expression is undetectable in the precartilage primordium contributing to the rod portion of Meckel's cartilage, whereas surrounding mesenchymal cells express *lacZ* (F). In the primordium of the rostral process of Meckel's cartilage, *lacZ* is highly expressed (H). Scale bars: 100 μm in A-C; 500 μm in D,G; 50 μm in E,F,H. aa2, second arch artery; as, aortic sac; da, dorsal aorta; dl, dental lamina; dm, dental mesenchyme; fg, foregut; gV, trigeminal ganglion; lj, lower jaw; nt, neural tube; pa1/2, first and second pharyngeal arches; pc, precartilage primordium of Meckel's cartilage; to, tongue; uj, upper jaw.

Knock-in of *Ednrb* cDNA could only partially rescue the *Ednra*-null phenotype

Previous studies have demonstrated that Edn1 can bind to both Ednra and Ednrb receptors with similar affinities and activate common signaling pathways, including G_q/G_{11}-dependent signals in many cells (Cramer et al., 2001; Jouneaux et al., 1994; Kedzierski and Yanagisawa, 2001; Masaki et al., 1999; Takigawa et al., 1995). If Ednra and Ednrb are interchangeable in the context of pharyngeal arch development, *Ednrb* knock-in is expected to rescue the Ednra-null phenotype. To test this possibility, we introduced *Ednrb* cDNA into the *Ednra*^{neo} allele in the same procedure as *Ednra* knock-in (Fig. 5A). Among 12 knock-in clones obtained through the screening, two clones were used to generate germline chimeras. Resultant heterozygous mice with the *Ednrb*-knock-in allele (*Ednra*^{B}) were intercrossed with *Ednra*$^{neo/+}$ or *Ednra*$^{lacZ/+}$ mice. The expression levels of *Ednrb* from the single knock-in allele were comparable to those of *Ednra* as estimated by RT-PCR analysis of E9.5 mandibular arches (Fig. 5A).

Unexpectedly, all the *Ednra*$^{neo/B}$ and *Ednra*$^{lacZ/B}$ mice died at birth and demonstrated craniofacial abnormalities similar to *Ednra*-null mice. In E18.5 *Ednra*$^{lacZ/B}$ mice, the appearance of the lower jaw was a mirror image of the upper jaw with vibrissae (Fig. 5C). Skeletal analysis of *Ednra*$^{lacZ/B}$ mice demonstrated a duplication of the upper jaw elements in the lower jaw region (Fig. 5E). Similar abnormalities were manifested in *Ednra*$^{B/B}$ mice, in which both of the two *Ednra* alleles were replaced with knocked-in *Ednrb* cDNA (data not shown).

The skeletal phenotype of *Ednra*$^{lacZ/B}$ and *Ednra*$^{B/B}$ mice, however, was different from that of *Ednra*-null mice in some respects. First, whereas the distal portion of the *Ednra*-null mandible was variable and often severely hypoplastic, failing to fuse at the midline (Fig. 4F,G), all the *Ednra*$^{lacZ/B}$ (n=7) and *Ednra*$^{B/B}$ (n=9) mice examined had relatively well-developed incisive alveolus, the appearance of which was similar to that of the normal dentary (Fig. 5E,F). Second, the hyoid in some *Ednrb*-knock-in mice was fused only unilaterally to the basisphenoid (in one of seven *Ednra*$^{lacZ/B}$ mice and four of nine *Ednra*$^{B/B}$ mice) or separated from the basisphenoid (in three of nine *Ednra*$^{B/B}$ mice), whereas all the *Ednra*$^{neo/neo}$ mice compared (n=10) showed bilateral hyoid-basisphenoid fusion. The hyoid in *Ednra*$^{lacZ/B}$ and *Ednra*$^{B/B}$ mice, whether it was fused to or separated from the basisphenoid, had nearly normal appearance compared with that of *Ednra*-null mice, although it typically had an extended ossification center and connected to the stapes though a transformed lesser horn as in *Ednra*$^{neo/neo}$ mice (Fig. 5G). Thirdly, ectopic cartilage appeared between the malleal/incal region and the extended basitrabecular process and/or ala temporalis in four of seven *Ednra*$^{lacZ/B}$ mice and six of nine *Ednra*$^{B/B}$ mice (Fig. 5H), whereas similar cartilage was observed in none of ten *Ednra*$^{neo/neo}$ mice (Fig. 4L). The first two differences may indicate that *Ednrb* can partially rescue the *Ednra*-null phenotype in the distal portion of the pharyngeal arch structures.

It has recently been reported that apoptotic cells are increased and extend distally in the mandibular arch mesenchyme of E9.5-10.5 *Ednra*-null embryos (Abe et al., 2007). To test whether knocked-in *Ednrb* could prevent increased apoptosis, we performed TUNEL staining on sections of E10.5 embryos. Consistently with the previous

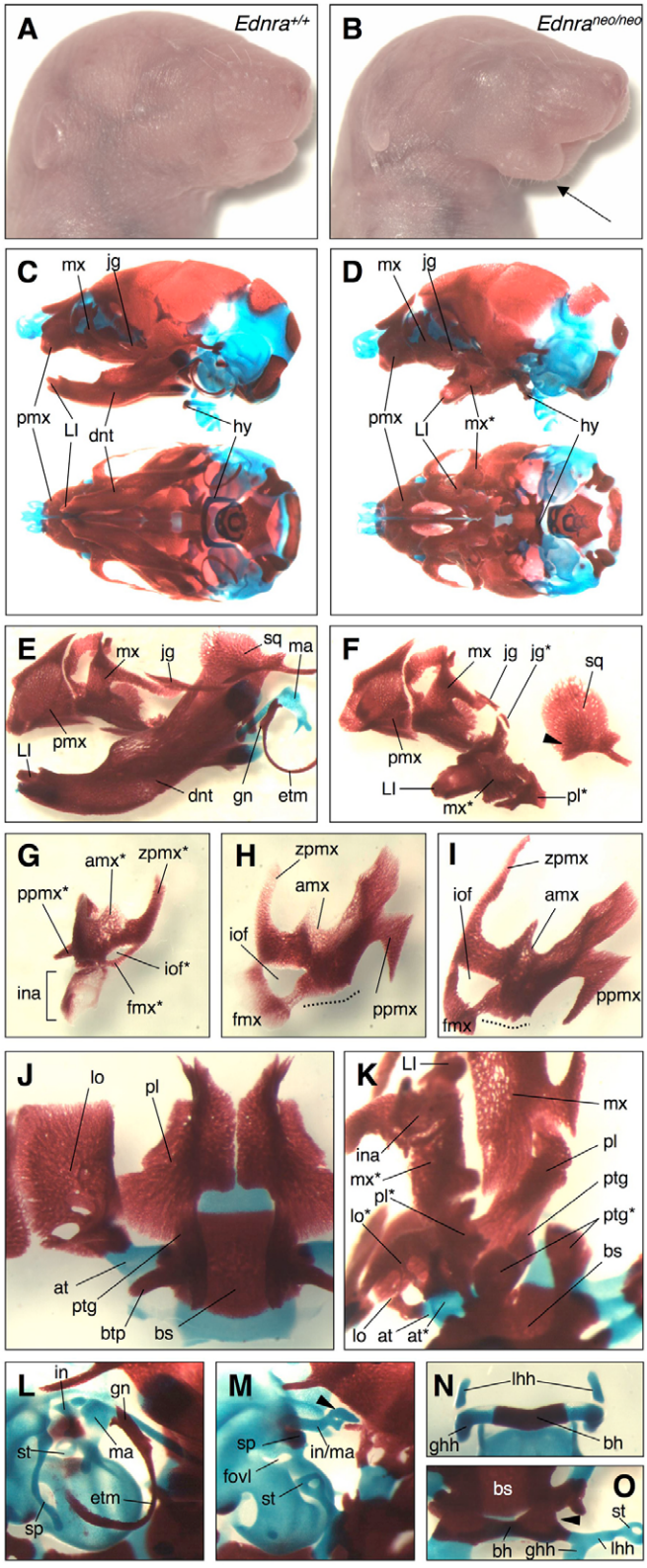

Fig. 4. Craniofacial defects of *Ednra*-null mice. Facial appearances (**A**,**B**) and skeletal structures (**C-O**) of E18.5 wild-type (A,C,E,I,J,L,N) and *Ednra*$^{neo/neo}$ (B,D,F-H,K,M,O) mice are shown. (A,B) The mutant lower jaw (arrow in B), in contrast to the normal one (A), appears a mirror image of the upper jaw with duplicated arrays of vibrissae. (C,D) Lateral and caudal views demonstrate defected and transformed mandibular (ventral) structures and malformed hyoid fused to the basisphenoid in mutants (D). (E,F) Mandibular elements including the dentary, goniale and ectotympanic (E) are mostly lost and replaced by ectopic structures resembling the maxilla, jugal and palatine, whereas the lower incisor with surrounding alveolar bone was formed in mutants (F). The zygomatic process of squamosal is often lost in mutants (arrowhead in F). (G-I) The ectopic bone in the mutant lower jaw (G) appears a duplication of the ipsilateral maxilla (H), which is almost identical to the wild-type one (I), except for the distal incisive alveolus. Broken lines in H and I indicate the margin articulating to the premaxilla. (J,K) A set of the palatine, pterygoid, ala temporalis and lamina obturans, the upper jaw elements in normal mice (J), are duplicated and connected to the ectopic maxilla (mx*) through palatomaxillary-like articulation in mutants (K). (L,M) In mutants, the malleus and incus are malformed, giving an ectopic structure extending to the squamosal (arrowhead in M). The stapes has nearly normal appearance, but is connected to the hyoid and displaced out of the fenestra ovalis (M). The styloid process was truncated in mutants (M). (N,O) Unlike the normal hyoid (N), the mutant hyoid is fused bilaterally to the basisphenoid (arrowhead in O) and connected to the stapes through an aberrant cartilageous strut (O). amx, alveolus of maxilla; at, ala temporalis; bh, body of hyoid; bs, basisphenoid; btp, basitrabecular process; dnt, dentary; etm, ectotympanic; fmx, frontal process of maxilla; fovl, fenestra ovalis; ghh, greater horn of hyoid; gn, goniale; hy, hyoid; in, incus; ina, incisive alveolus of dentary; iof, infraorbital foramen; jg, jugal; lhh, lesser horn of hyoid; LI, lower incisor; lo, lamina obturans; ma, malleus; mx, maxilla; pl, palatine; pmx, premaxilla, ppmx, palatal process of maxilla; ptg, pterygoid; sp, styloid process; sq, squamosal; st, stapes; zpmx, zygomatic process of maxilla; *, ectopic structure.

report, TUNEL-positive cells extended from the proximal to the distal mandibular region in E10.5 *Ednra*$^{neo/neo}$ embryos (n=5), whereas TUNEL-positive cells were confined to the proximal region in wild-type embryos (n=6) (Fig. 6A,B). Similarly, *Ednra*$^{neo/B}$ embryos also showed apparently increased numbers of TUNEL-positive cells extending into the distal mandibular region (n=4) (Fig. 6C).

We further examined gene expression profiles in *Ednrb*-knock-in embryos by whole-mount in situ hybridization. *LacZ* signals were equally distributed within the pharyngeal arch region in E9.5 control, *Ednra*$^{lacZ/B}$ (Fig. 7A,B) and *Ednra*-null (data not shown) embryos, suggesting that *Ednra*-positive cells were present there to a similar extent. In the pharyngeal arch mesenchyme of E9.5 *Ednra*$^{B/B}$ embryos, the expression of *Dlx3*, *Dlx5* and *Dlx6* is downregulated (Fig. 7C-H), as in *Edn1*$^{-/-}$ and *Ednra*$^{-/-}$ embryos (Charite et al., 2001; Clouthier et al., 2000; Ozeki et al., 2004). The expression of *Hand2* and *Goosecoid* was also downregulated in *Ednra*$^{B/B}$ pharyngeal arches (Fig. 7I-L), as in *Edn1*$^{-/-}$ and *Ednra*$^{-/-}$ embryos (Clouthier et al., 1998; Thomas et al., 1998) as well as in *Dlx5*$^{-/-}$;*Dlx6*$^{-/-}$ embryos (Charite et al., 2001; Depew et al., 1999; Depew et al., 2002). Taken together with morphological and apoptosis analysis, these results indicate that Ednrb cannot substitute for Ednra in pharyngeal development, although it may partially rescue the *Ednra*-null phenotype.

Comparison of craniofacial structures between *Ednra*-modified mice and neural-crest-specific $G\alpha_q/G\alpha_{11}$-deficient mice

Offermanns's group has demonstrated that *P0-Cre*$^{-/+}$;*G*$\alpha_q^{flox/flox}$;*G*$\alpha_{11}^{-/-}$ mice lacking $G\alpha_q/G\alpha_{11}$ in a neural-crest-specific manner show craniofacial defects similar to those in *Edn1*- or *Ednra*-deficient mice (Dettlaff-Swiercz et al., 2005). However,

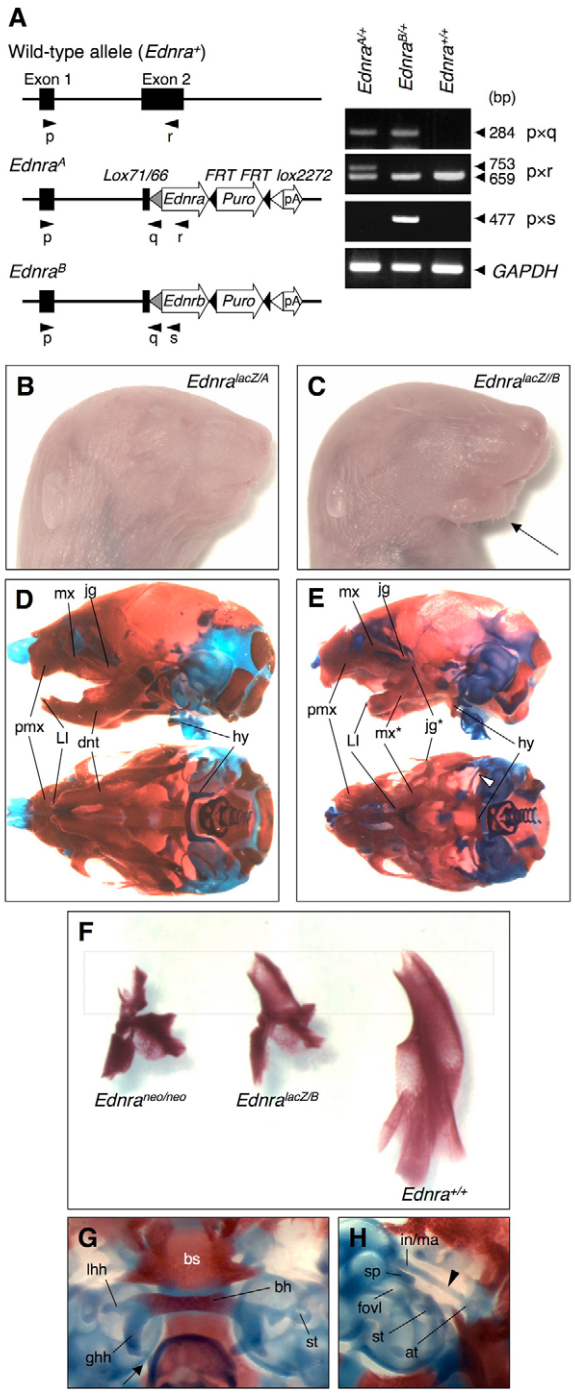

Fig. 5. Phenotypes of *Ednra* and *Ednrb* knock-in mice. (**A**) RMCE-mediated knock-in of *Ednra* and *Ednrb* cDNA into the *Ednra* locus. Partial structures of the wild-type and knocked-in *Ednra* allele and RT-PCR analysis for the expression of knocked-in genes in mandibular arches of E9.5 *Ednra*- and *Ednrb*-knock-in heterozygous embryos are shown. PCR primers were represented by arrowheads in the left panel. Note that 753- and 659-bp bands correspond to knocked-in and endogenous *Ednra* transcripts, respectively. (**B-H**) Facial appearances (B,C) and skeletal structures (D-H) of E18.5 $Ednra^{lacZ/A}$ (*Ednra*-knock-in) (B,D) and $Ednra^{lacZ/B}$ (*Ednrb*-knock-in) (C,E-H) mice. *Ednra* knock-in restored normal facial appearance (B) and skeletal structures (D). *Ednrb* knock-in mice still exhibit craniofacial defects resembling the *Ednra*-null phenotype (C,E), except for some differences described below. White arrowhead, ectopic cartilage connecting the incus and extended basitrabecular process. (F) Comparison of the morphology of incisive alveolar bones (boxed with dotted line) among the *Ednra*-null ($Ednra^{neo/neo}$), *Ednrb*-knock-in ($Ednra^{lacZ/B}$) and wild-type ($Ednra^{+/+}$) mandible. Incisors were removed. The $Ednra^{lacZ/B}$ incisive alveolus is well developed, comparable with the wild-type one. (G) A representative of the $Ednra^{B/B}$ hyoid, which is, unlike the *Ednra*-null hyoid, not fused to the basisphenoid. The body has an extended ossification center and is connected to the stapes though a transformed lesser horn. The great horn is fused with the superior horn of the thyroid (arrow). (H) Ectopic cartilage (arrowhead) between the malleal/incal region and ala temporalis in $Ednra^{lacZ/B}$ mice. at, ala temporalis; bh, body of hyoid; bs, basisphenoid; dnt, dentary; fovl, fenestra ovalis; ghh, greater horn of hyoid; hy, hyoid; in, incus; jg, jugal; lhh, lesser horn of hyoid; LI, lower incisor; ma, malleus; mx, maxilla; pmx, premaxilla, sp, styloid process; st, stapes; zpmx, zygomatic process of maxilla; *, ectopic structure.

detailed description in terms of this similarity has not yet been reported. To clarify the relationship between Edn receptors and $G\alpha_q/G\alpha_{11}$ signaling in neural-crest-derived ectomesenchyme, we revisited the craniofacial phenotype of neural-crest-specific $G\alpha_q/G\alpha_{11}$-deficient mice.

In addition to the duplication of the jugal and maxillary bones in the mandibular region, $G\alpha_q/G\alpha_{11}$-deficient mice had duplicated palatine, pterygoid and lamina obturans (Fig. 8A-D), as observed in *Ednra*-null (Fig. 4D,F) and *Ednrb*-knock-in (Fig. 5E, Fig. 8E) mice. Unlike *Ednra*-null mice, however, the incisive alveolar bone in the distal mandibular region was relatively well developed in all the $G\alpha_q/G\alpha_{11}$-deficient mice examined (n=8) (Fig. 8B,D,F). This morphological feature is reminiscent of the *Ednrb*-knock-in phenotype (Fig. 8E,G) rather than the *Ednra*-null one (Fig. 8H). The basitrabecular process was abnormally extended to the ear region in all the cases (Fig. 8B,D). Furthermore, the hyoid of $G\alpha_q/G\alpha_{11}$-deficient mice was not fused to the basisphenoid in all the cases (Fig. 8I,J). Instead, the body has an extended ossification center and is fused with the lesser horn and often with the superior horn of the thyroid (Fig. 8I,J), as seen in *Ednrb*-knock-in mice (Fig. 5G). These similarities suggest that $G\alpha_q/G\alpha_{11}$ mainly mediate Ednra-selective signaling in neural-crest-derived mesenchyme during pharyngeal arch development, but the Ednrb-replaceable signaling is likely to be mediated by the $G\alpha_q/G\alpha_{11}$-independent pathway.

DISCUSSION

Previous studies have implicated Edn1/Ednra signaling as a mediator of regional specification and morphogenesis in craniofacial development in vertebrates. To further investigate the intracellular mechanism underlying the involvement of the Edn1/Ednra signaling in embryonic development, we adopted RMCE using the Cre-*lox* system to introduce genes of interest into the *Ednra* locus in mouse ES cells systematically and efficiently. Indeed, the efficiency of RMCE-mediated knock-in recombination was very high in our screening (44 to 87%), compared with conventional homologous recombination. This is similar to or higher than the efficiencies previously reported for RMCE using the Cre-*lox* system (Araki et al., 2006; Liu et al., 2006; Toledo et al., 2006) or the Flp-*FRT* system (Cesari et al., 2004; Roebroek et al., 2006). In our RMCE procedure, we replaced a 1.0 kb genomic sequence with knock-in sequences containing mutant *lox* sites and an *FRT*-flanked *Puro*. The expression of knocked-in *lacZ* appeared to recapitulate endogenous

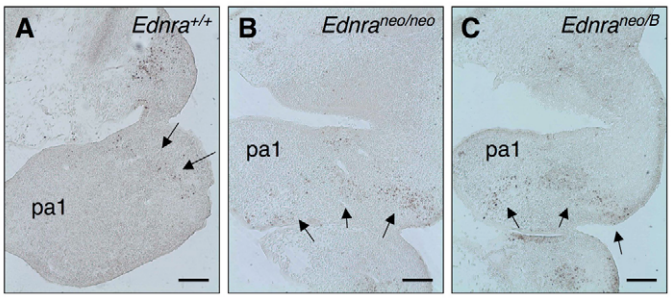

Fig. 6. Apoptosis analysis. TUNEL staining of E10.5 transverse sections through the mandibular arch reveals that TUNEL-positive cells (arrows) are confined to the proximal region in wild-type mouse embryos (**A**), but extend widely into the distal arch region in *Ednra*$^{neo/neo}$ (**B**) and *Ednra*$^{neo/B}$ (**C**) embryos. Scale bars: 100 μm. pa1, first pharyngeal (mandibular) arch.

Ednra expression irrespective of the presence of *Puro*, and the knock-in of *Ednra* cDNA could normalize craniofacial defects caused by *Ednra*-null mutation. Furthermore, no additional abnormalities were evident in any knock-in mice after RMCE procedure at least in terms of embryonic development, viability and fertility. These results support the relevance of our RMCE-mediated knock-in procedure for analysis of gene function in craniofacial development.

Ednra-lacZ expression in the head mesenchyme and cranial neural crest derivatives

Previous studies have indicated that Edn1 acts on cranial/cardiac neural crest cells through Ednra and activates transcriptional machinery responsible for dorsoventral patterning (Charite et al., 2001; Ozeki et al., 2004; Ruest et al., 2004). The crucial window for this Edn1-Ednra interaction in pharyngeal arch development is around E8.5 to 9.0, when regional identities start to be specified within the anterior pharyngeal arches (Fukuhara et al., 2004). Consistently, *Ednra-lacZ* expression was detectable just before this stage (E8.25; ~6-somite stage) in the head mesenchyme including migratory neural crest cells delaminating from the dorsal neuroepithelium. By contrast, premigratory neural crest cells in the neural plate did not express *lacZ*, suggesting that the induction of *Ednra* expression may be coupled with epithelial-mesenchymal transition. Thereafter, *Ednra*-expressing neural crest cells migrating into the ventral region of the anterior pharyngeal arches are supposed to receive the Edn1 signal, leading to the upregulation of *Dlx5*/*Dlx6* expression and the specification of a ventral identity.

In addition to the expression in neural-crest-derived mesenchymal cells, *Ednra-lacZ* was likely to be expressed in the mesoderm-derived head mesenchyme. This is further supported by the difference in the pattern of *lacZ* expression between the *Ednra-lacZ* mice and other mice in which neural crest cells are specifically marked. *Protein 0* (*P0*)-*Cre* transgenic mice harboring a conditional *lacZ* allele, for example, demonstrated *lacZ* expression broadly in neural-crest derivatives (Yamauchi et al., 1999). The *Wnt1-Cre* transgene also directed the expression of a conditional *lacZ* allele specifically to neural crest cells in mice (Chai et al., 2000). In both cases, the head mesenchyme adjacent to the neural tube was largely *lacZ*-negative. In fact, the head mesenchyme originated from both the cranial paraxial mesoderm and neural crest (Trainor and Tam, 1995). Thus, *Ednra* appears to be extensively expressed in mesoderm-derived mesenchyme (except for the pharyngeal core mesoderm and vascular endothelium) as well as in neural-crest-derived ectomesenchyme in the craniofacial region.

At later stages, *Ednra-lacZ* expression was observed in many cranial/cardiac neural crest derivatives. In the Meckel's cartilage primordium, which is also derived from neural crest cells, *lacZ* expression was detected only in the rostral process, a distalmost portion, at E12.5. At E12.5 to 13.5, the rostral process is rich in proliferative, undifferentiated cells, while cells start to differentiate into chondrocytes in the bilateral rod portion (Ramaesh and Bard, 2003). Thus, *Ednra* expression in neural-crest derivatives may be stage- and/or lineage-dependent.

Diversity of Edn receptor signaling in pharyngeal arch development

Ednra and Ednrb share common ligand affinities and downstream signaling pathways. In particular, the G_q/G_{11}-mediated pathway, which is assumed to be responsible for Edn1/Ednra-dependent craniofacial development, is also activated by Ednrb stimulation in various cell types (Cramer et al., 2001; Jouneaux et al., 1994; Masaki et al., 1999; Takigawa et al., 1995). However, knock-in of *Ednrb* failed to rescue homeotic transformation of the lower jaw into

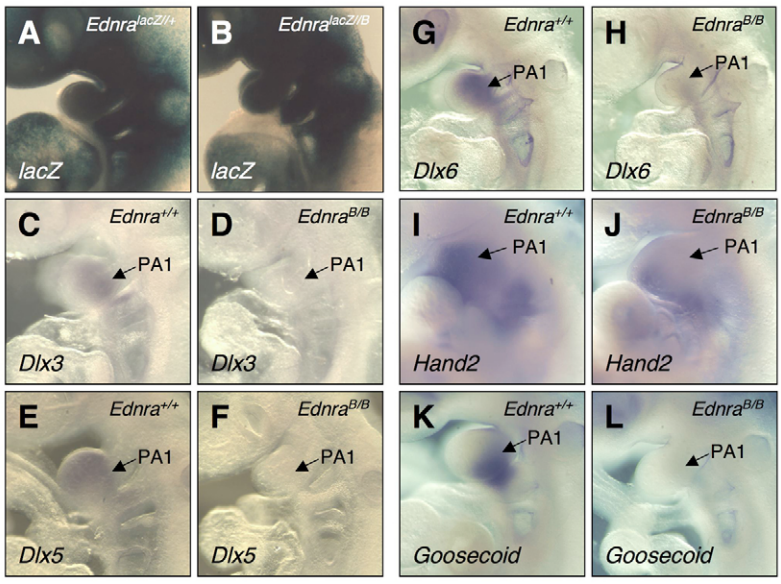

Fig. 7. Gene expression analysis of the pharyngeal arches in *Ednrb*-knock-in embryos. (**A**,**B**) Whole-mount *lacZ* staining of E10.5 *Ednra*$^{lacZ/+}$ (A) and *Ednra*$^{lacZ/B}$ (B) mouse embryos. (**C-L**) Whole-mount in situ hybridization for *Dlx3* (C,D), *Dlx5* (E,F), *Dlx6* (G,H), *Hand2* (I,J) and *Goosecoid* (K,L) in wild-type (C,E,G,I,K) and *Ednra*$^{B/B}$ (D,F,H,J,L) embryos at E9.5 (C-H), E10.0 (K,L) or E10.5 (I,J). The expression of *Dlx3*, *Dlx5*, *Dlx6*, *Hand2* and *Goosecoid* was downregulated in *Ednra*$^{B/B}$ arches.

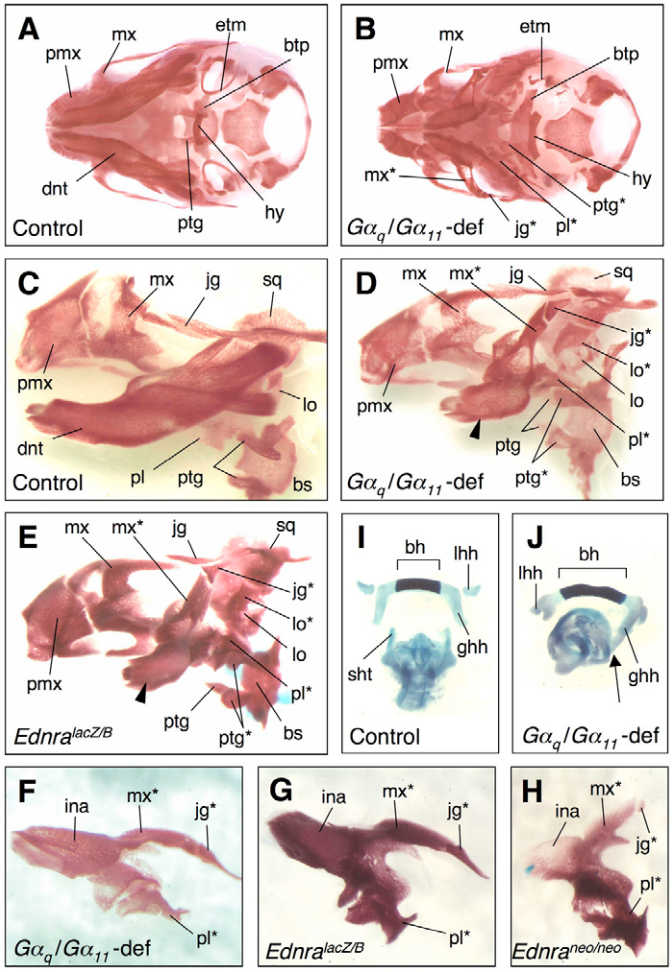

Fig. 8. Craniofacial defects of neural-crest-specific $G\alpha_q/G\alpha_{11}$-deficient mice. (**A-E**) Skeletal structures of E18.5 *P0-Cre*$^{-/-}$;*Gα*$_q^{flox/flox}$;*Gα*$_{11}^{-/-}$ (control) (A,C), *P0-Cre*$^{-/+}$;*Gα*$_q^{flox/flox}$;*Gα*$_{11}^{-/-}$ ($G\alpha_q/G\alpha_{11}$-deficient) (B,D) and *Ednra*$^{lacZ/B}$ (E) mice. $G\alpha_q/G\alpha_{11}$-deficient mice have a duplicated set of the maxilla, jugal, palatine, pterygoid and lamina obturans, and relatively well-developed incisive alveolus in the distal mandibular region (arrowheads), as *Ednra*$^{lacZ/B}$ mice. (**F-H**) Transformed mandibular components (ectopic maxilla, jugal and palatine bones) of $G\alpha_q/G\alpha_{11}$-deficient (F), *Ednra*$^{lacZ/B}$ (G) and *Ednra*$^{neo/neo}$ (H) mice. (**I**,**J**) Hyoid and thyroid cartilages of control (I) and $G\alpha_q/G\alpha_{11}$-deficient (J) mice. Unlike *Ednra*-null hyoid, the $G\alpha_q/G\alpha_{11}$-deficient hyoid is not fused to the basisphenoid. Instead, the body has an extended ossification center and is fused with the lesser horn of the hyoid and the superior horn of the thyroid (arrow). bh, body of hyoid; bs, basisphenoid; btp, basitrabecular process; dnt, dentary; etm, ectotympanic; ghh, greater horn of hyoid; hy, hyoid; ina, incisive alveolus of dentary; jg, jugal; lhh, lesser horn of hyoid; lo, lamina obturans; mx, maxilla; pl, palatine; pmx, premaxilla; ptg, pterygoid; sht, superior horn of the thyroid; sq, squamosal; *, ectopic structure.

an upper jaw-like structure in *Ednra*-null mice, although knocked-in *Ednrb* appeared to be expressed at levels similar to those of knocked-in *Ednra*. This result indicates that Ednrb cannot restore Ednra function in the specification of mandibular identity in pharyngeal arch development.

One possible explanation for the failure of rescue by *Ednrb* knock-in is that Ednrb might not activate G_q/G_{11} adequately enough to elicit downstream signals necessary for the ventral specification of the

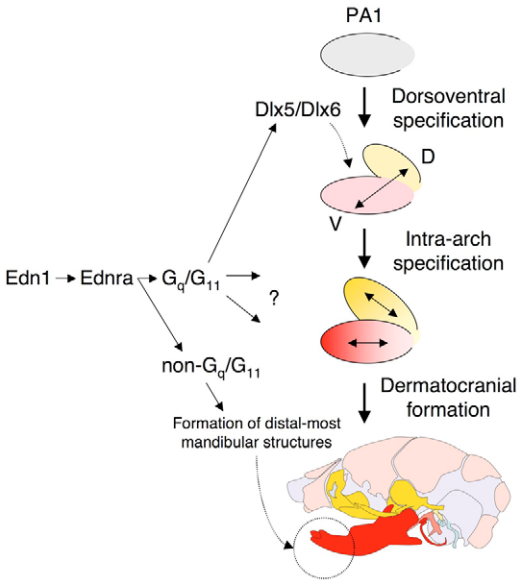

Fig. 9. Scheme illustrating the possible role of G_q/G_{11}-dependent and -independent Edn1/Ednra signaling in pharyngeal arch development.

pharyngeal arches. Indeed, Ednrb is less potent in G_q coupling in some cells and in reconstituted phospholipid vesicles (Doi et al., 1999; Takigawa et al., 1995). It is also possible that Ednrb may not associate with G_q/G_{11} in cranial neural crest cells in a physiological context. In trunk neural crest development giving rise to the enteric nerve system, the Edn3/Ednrb signal is likely to be mediated by inhibition of protein kinase A (Barlow et al., 2003), which appears to be independent of G_q/G_{11}. Thus, Ednra and Ednrb may couple to different G proteins, leading to activation of distinct signaling pathways. Another possibility is that difference in receptor desensitization or differences in the potency and/or efficacy of the receptor agonists with regard to receptor activation might cause the failure of rescue by *Ednrb*. Further studies are required to test these possibilities.

By contrast, there were some differences in craniofacial defects between *Ednra*-null and *Ednrb* knock-in mice. Unlike *Ednra*-null mice, *Ednrb* knock-in mice had a relatively well-developed incisive alveolar bone of the mandible and, in some cases, the hyoid separated from the basisphenoid as in normal mice. Extended basitrabecular process with connection to ectopic cartilage was often observed in *Ednrb* knock-in mice. The first two differences suggest that Ednrb may partially replace Ednra function in the development of distal structures in the mandibular and hyoid arches. Considering the regional heterogeneity in *Ednra* expression within the Meckel's primordium, the Edn1/Ednra signal may be also required for the formation of the distal region later than the stage of dorsoventral specification. Interestingly, craniofacial defects of neural-crest-specific $G\alpha_q/G\alpha_{11}$-deficient mice were very similar to those of *Ednrb* knock-in mice rather than *Ednra*-null mice. This similarity suggests that aspects of the Edn1/Ednra signaling that Ednrb can substitute may be mediated by a G_q/G_{11}-independent pathway. Thus, Edn1/Ednra may activate different G proteins in different contexts during pharyngeal arch development. Alternatively, Edn receptor functions in cells other than the neural-crest derivatives may also be required for pharyngeal arch development. The mechanism underlying the selectivity of the Edn receptors in terms of G-protein coupling in cranial neural crest cells in different contexts should be clarified in further investigations.

Regionality within the mandible in terms of the requirement for Edn1/Ednra-G_q/G_{11} signaling

The present study showed that the proximal portion of the dentary underwent homeotic transformation into upper jaw elements, whereas the distal portion maintained its mandibular identity in *Ednra*-null, *Ednrb*-knock-in and $G\alpha_q/G\alpha_{11}$-null mice. Notably, the ectopic bone replacing the dentary in mutant mice resembled the maxilla, leaving incisive alveolar bone with mandibular identity in the distal portion. Thus, the proximal region of the dentary requires the Edn1/Ednra to G_q/G_{11} signaling for establishing its mandibular identity, and this signaling cannot be replaced by Ednrb. Dlx5 and Dlx6 are likely to be activated by this pathway, because the expression of *Dlx5*, *Dlx6* and their downstream genes was downregulated in the mandible of *Ednrb*-knock-in mice as well as $G\alpha_q/G\alpha_{11}$-deficient mice (Ivey et al., 2003). Increased apoptosis extending to the distal mandibular arch may also be related to defects in this pathway, although apoptosis in $G\alpha_q/G\alpha_{11}$-deficient mice has not yet been analyzed. By contrast, this signaling pathway is dispensable for the mandibular identity of the distal incisive alveolus. G_q/G_{11}-independent Ednra signaling, which can be replaced by *Ednrb* knock-in, may contribute to the growth of this portion. It has previously been shown that neural-crest-specific $G\alpha_{12}/G\alpha_{13}$-deficient mice have no craniofacial defects, making it unlikely that G_{12}/G_{13} are involved (Dettlaff-Swiercz et al., 2005). Thus, other types of trimeric G proteins such as G_i/G_o may be involved in this pathway. The possible dual roles of the Edn1/Ednra signaling in pharyngeal arch development are summarized in Fig. 9.

The incisive alveolus appears to be equivalent to the premaxilla in the upper jaw, as extrapolated from the conjunction to the maxillary(-like) bone in *Ednra*-null mutants (Fig. 4G,H). This portion and the premaxilla are missing in *Dlx5/6*$^{-/-}$ mice, indicating that these structures are dependent on Dlx5 and Dlx6 (Beverdam et al., 2002; Depew et al., 2002). Residual *Dlx5* and *Dlx6*, independent of the Edn1/Ednra to G_q/G_{11} signaling, may be responsible for the formation of these distal structures.

Usefulness of the present RMCE-mediated knock-in system in studies on craniofacial development

The present RMCE-mediated knock-in procedure enabled us to introduce a series of gene cassettes to be expressed in a spatiotemporal pattern similar to the endogenous *Ednra*. The efficiency was much higher than that of conventional homologous recombination in ES cells. Using this procedure, we could examine the expression pattern and function of Ednra in craniofacial development. In particular, differences in *Ednra* and *Ednrb* knock-in have provided a clue to further analysis of the receptor domain function. Furthermore, this system can be broadly applicable for studies on gene function, including cell fate determination, differentiation, regional specification and so on. These applications will largely contribute to our understanding of the molecular mechanisms that regulate craniofacial development.

We thank Ken-ichi Yamamura and Kimi Araki (Kumamoto University) for plasmids containing mutant lox sequence, Izumu Saito (University of Tokyo) for Cre-expressing adenovirus, Deepak Srivastava (University of California, San Francisco) and Gen Yamada (Kumamoto University) for probes, Makoto Abe (Osaka University) for technical advice, Nanako Hoya, Yuko Fujisawa, Sakura Kushiyama and Seiko Ito for technical assistance, Fumihiko Ikemoto, Masaru Nishikibe and colleagues in Banyu Pharmaceutical Co., Ltd. for supporting this work. This work was supported by grants-in-aid for scientific research from the Ministry of Education, Culture, Sports, Science and Technology, Japan, and grants-in-aid for scientific research from the Ministry of Health, Labour and Welfare of Japan.

References

Abe, M., Ruest, L. B. and Clouthier, D. E. (2007). Fate of cranial neural crest cells during craniofacial development in endothelin-A receptor-deficient mice. *Int. J. Dev. Biol.* **51**, 97-105.

Araki, K., Araki, M. and Yamamura, K. (2002). Site-directed integration of the cre gene mediated by Cre recombinase using a combination of mutant lox sites. *Nucleic Acids Res.* **30**, e103.

Araki, K., Araki, M. and Yamamura, K. (2006). Negative selection with the Diphtheria toxin A fragment gene improves frequency of Cre-mediated cassette exchange in ES cells. *J. Biochem.* **140**, 793-798.

Barlow, A., de Graaff, E. and Pachnis, V. (2003). Enteric nervous system progenitors are coordinately controlled by the G protein-coupled receptor EDNRB and the receptor tyrosine kinase RET. *Neuron* **40**, 905-916.

Beverdam, A., Merlo, G. R., Paleari, L., Mantero, S., Genova, F., Barbieri, O., Janvier, P. and Levi, G. (2002). Jaw transformation with gain of symmetry after Dlx5/Dlx6 inactivation: mirror of the past? *Genesis* **34**, 221-227.

Cesari, F., Rennekampff, V., Vintersten, K., Vuong, L. G., Seibler, J., Bode, J., Wiebel, F. F. and Nordheim, A. (2004). Elk-1 knock-out mice engineered by Flp recombinase-mediated cassette exchange. *Genesis* **38**, 87-92.

Chai, Y. and Maxson, R. E., Jr (2006). Recent advances in craniofacial morphogenesis. *Dev. Dyn.* **235**, 2353-2375.

Chai, Y., Jiang, X., Ito, Y., Bringas, P., Jr, Han, J., Rowitch, D. H., Soriano, P., McMahon, A. P. and Sucov, H. M. (2000). Fate of the mammalian cranial neural crest during tooth and mandibular morphogenesis. *Development* **127**, 1671-1679.

Charite, J., McFadden, D. G., Merlo, G., Levi, G., Clouthier, D. E., Yanagisawa, M., Richardson, J. A. and Olson, E. N. (2001). Role of Dlx6 in regulation of an endothelin-1-dependent, dHAND branchial arch enhancer. *Genes Dev.* **15**, 3039-3049.

Clouthier, D. E., Hosoda, K., Richardson, J. A., Williams, S. C., Yanagisawa, H., Kuwaki, T., Kumada, M., Hammer, R. E. and Yanagisawa, M. (1998). Cranial and cardiac neural crest defects in endothelin-A receptor-deficient mice. *Development* **125**, 813-824.

Clouthier, D. E., Williams, S. C., Yanagisawa, H., Wieduwilt, M., Richardson, J. A. and Yanagisawa, M. (2000). Signaling pathways crucial for craniofacial development revealed by endothelin-A receptor-deficient mice. *Dev. Biol.* **217**, 10-24.

Cramer, H., Schmenger, K., Heinrich, K., Horstmeyer, A., Boning, H., Breit, A., Piiper, A., Lundstrom, K., Muller-Esterl, W. and Schroeder, C. (2001). Coupling of endothelin receptors to the ERK/MAP kinase pathway. Roles of palmitoylation and G(alpha)q. *Eur. J. Biochem.* **268**, 5449-5459.

Depew, M. J., Liu, J. K., Long, J. E., Presley, R., Meneses, J. J., Pedersen, R. A. and Rubenstein, J. L. (1999). Dlx5 regulates regional development of the branchial arches and sensory capsules. *Development* **126**, 3831-3846.

Depew, M. J., Lufkin, T. and Rubenstein, J. L. (2002). Specification of jaw subdivisions by Dlx genes. *Science* **298**, 381-385.

Depew, M. J., Simpson, C. A., Morasso, M. and Rubenstein, J. L. (2005). Reassessing the Dlx code: the genetic regulation of branchial arch skeletal pattern and development. *J. Anat.* **207**, 501-561.

Dettlaff-Swiercz, D. A., Wettschureck, N., Moers, A., Huber, K. and Offermanns, S. (2005). Characteristic defects in neural crest cell-specific Galphaq/Galpha11- and Galpha12/Galpha13-deficient mice. *Dev. Biol.* **282**, 174-182.

Doi, T., Sugimoto, H., Arimoto, I., Hiroaki, Y. and Fujiyoshi, Y. (1999). Interactions of endothelin receptor subtypes A and B with Gi, Go, and Gq in reconstituted phospholipid vesicles. *Biochemistry* **38**, 3090-3099.

Fukuhara, S., Kurihara, Y., Arima, Y., Yamada, N. and Kurihara, H. (2004). Temporal requirement of signaling cascade involving endothelin-1/endothelin receptor type A in branchial arch development. *Mech. Dev.* **121**, 1223-1233.

Ivey, K., Tyson, B., Ukidwe, P., McFadden, D. G., Levi, G., Olson, E. N., Srivastava, D. and Wilkie, T. M. (2003). Galphaq and Galpha11 proteins mediate endothelin-1 signaling in neural crest-derived pharyngeal arch mesenchyme. *Dev. Biol.* **255**, 230-237.

Jouneaux, C., Mallat, A., Serradeil-Le Gal, C., Goldsmith, P., Hanoune, J. and Lotersztajn, S. (1994). Coupling of endothelin B receptors to the calcium pump and phospholipase C via Gs and Gq in rat liver. *J. Biol. Chem.* **269**, 1845-1851.

Kanegae, Y., Lee, G., Sato, Y., Tanaka, M., Nakai, M., Sakaki, T., Sugano, S. and Saito, I. (1995). Efficient gene activation in mammalian cells by using recombinant adenovirus expressing site-specific Cre recombinase. *Nucleic Acids Res.* **23**, 3816-3821.

Kedzierski, R. M. and Yanagisawa, M. (2001). Endothelin system: the double-edged sword in health and disease. *Annu. Rev. Pharmacol. Toxicol.* **41**, 851-876.

Kempf, H., Linares, C., Corvol, P. and Gasc, J. M. (1998). Pharmacological inactivation of the endothelin type A receptor in the early chick embryo: a model of mispatterning of the branchial arch derivatives. *Development* **125**, 4931-4941.

Kimmel, C. B., Ullmann, B., Walker, M., Miller, C. T. and Crump, J. G. (2003). Endothelin 1-mediated regulation of pharyngeal bone development in zebrafish. *Development* **130**, 1339-1351.

Kontges, G. and Lumsden, A. (1996). Rhombencephalic neural crest

segmentation is preserved throughout craniofacial ontogeny. *Development* **122**, 3229-3242.
Kurihara, Y., Kurihara, H., Suzuki, H., Kodama, T., Maemura, K., Nagai, R., Oda, H., Kuwaki, T., Cao, W. H., Kamada, N. et al. (1994). Elevated blood pressure and craniofacial abnormalities in mice deficient in endothelin-1. *Nature* **368**, 703-710.
Kurihara, Y., Kurihara, H., Oda, H., Maemura, K., Nagai, R., Ishikawa, T. and Yazaki, Y. (1995). Aortic arch malformations and ventricular septal defect in mice deficient in endothelin-1. *J. Clin. Invest.* **96**, 293-300.
Kurihara, H., Kurihara, Y., Nagai, R. and Yazaki, Y. (1999). Endothelin and neural crest development. *Cell. Mol. Biol. (Noisy-le-grand)* **45**, 639-651.
Le Douarin, N. M. and Kalcheim, C. (1999). *The Neural Crest* (2nd edn). Cambridge: Cambridge University Press.
Liu, K., Hipkens, S., Yang, T., Abraham, R., Zhang, W., Chopra, N., Knollmann, B., Magnuson, M. A. and Roden, D. M. (2006). Recombinase-mediated cassette exchange to rapidly and efficiently generate mice with human cardiac sodium channels. *Genesis* **44**, 556-564.
Maemura, K., Kurihara, H., Kurihara, Y., Oda, H., Ishikawa, T., Copeland, N. G., Gilbert, D. J., Jenkins, N. A. and Yazaki, Y. (1996). Sequence analysis, chromosomal location, and developmental expression of the mouse preproendothelin-1 gene. *Genomics* **31**, 177-184.
Masaki, T. (2004). Historical review: endothelin. *Trends Pharmacol. Sci.* **25**, 219-224.
Masaki, T., Ninomiya, H., Sakamoto, A. and Okamoto, Y. (1999). Structural basis of the function of endothelin receptor. *Mol. Cell. Biochem.* **190**, 153-156.
McLeod, M. J. (1980). Differential staining of cartilage and bone in whole mouse fetuses by alcian blue and alizarin red S. *Teratology* **22**, 299-301.
Merlo, G. R., Zerega, B., Paleari, L., Trombino, S., Mantero, S. and Levi, G. (2000). Multiple functions of Dlx genes. *Int. J. Dev. Biol.* **44**, 619-626.
Miller, C. T., Schilling, T. F., Lee, K., Parker, J. and Kimmel, C. B. (2000). sucker encodes a zebrafish Endothelin-1 required for ventral pharyngeal arch development. *Development* **127**, 3815-3828.
Nagy, A., Gertsenstein, M., Vintersten, K. and Behringer, R. (2003). *Manipulating the Mouse Embryo: A Laboratory Manual* (3rd edn). Cold Spring Harbor: Cold Spring Harbor Laboratory Press.
Nieto, M. A., Bennett, M. F., Sargent, M. G. and Wilkinson, D. G. (1992). Cloning and developmental expression of Sna, a murine homologue of the Drosophila snail gene. *Development* **116**, 227-237.
Noden, D. M. and Trainor, P. A. (2005). Relations and interactions between cranial mesoderm and neural crest populations. *J. Anat.* **207**, 575-601.
Offermanns, S., Zhao, L. P., Gohla, A., Sarosi, I., Simon, M. I. and Wilkie, T. M. (1998). Embryonic cardiomyocyte hypoplasia and craniofacial defects in G alpha q/G alpha 11-mutant mice. *EMBO J.* **17**, 4304-4312.
Ozeki, H., Kurihara, Y., Tonami, K., Watatani, S. and Kurihara, H. (2004). Endothelin-1 regulates the dorsoventral branchial arch patterning in mice. *Mech. Dev.* **121**, 387-395.
Ramaesh, T. and Bard, J. B. (2003). The growth and morphogenesis of the early mouse mandible: a quantitative analysis. *J. Anat.* **203**, 213-222.
Roebroek, A. J., Reekmans, S., Lauwers, A., Feyaerts, N., Smeijers, L. and Hartmann, D. (2006). Mutant Lrp1 knock-in mice generated by recombinase-mediated cassette exchange reveal differential importance of the NPXY motifs in the intracellular domain of LRP1 for normal fetal development. *Mol. Cell. Biol.* **26**, 605-616.
Ruberte, E., Friederich, V., Morriss-Kay, G. and Chambon, P. (1992). Differential distribution patterns of CRABP I and CRABP II transcripts during mouse embryogenesis. *Development* **115**, 973-987.
Ruest, L. B., Xiang, X., Lim, K. C., Levi, G. and Clouthier, D. E. (2004). Endothelin-A receptor-dependent and -independent signaling pathways in establishing mandibular identity. *Development* **131**, 4413-4423.
Schlake, T. and Bode, J. (1994). Use of mutated FLP recognition target (FRT) sites for the exchange of expression cassettes at defined chromosomal loci. *Biochemistry* **33**, 12746-12751.
Smith, D. E., Franco del Amo, F. and Gridley, T. (1992). Isolation of Sna, a mouse gene homologous to the Drosophila genes snail and escargot: its expression pattern suggests multiple roles during postimplantation development. *Development* **116**, 1033-1039.
Sorrell, D. A. and Kolb, A. F. (2005). Targeted modification of mammalian genomes. *Biotechnol. Adv.* **23**, 431-469.
Spence, S., Anderson, C., Cukierski, M. and Patrick, D. (1999). Teratogenic effects of the endothelin receptor antagonist L-753,037 in the rat. *Reprod. Toxicol.* **13**, 15-29.
Srivastava, D., Cserjesi, P. and Olson, E. N. (1995). A subclass of bHLH proteins required for cardiac morphogenesis. *Science* **270**, 1995-1999.
Takigawa, M., Sakurai, T., Kasuya, Y., Abe, Y., Masaki, T. and Goto, K. (1995). Molecular identification of guanine-nucleotide-binding regulatory proteins which couple to endothelin receptors. *Eur. J. Biochem.* **228**, 102-108.
Thomas, T., Kurihara, H., Yamagishi, H., Kurihara, Y., Yazaki, Y., Olson, E. N. and Srivastava, D. (1998). A signaling cascade involving endothelin-1, dHAND and msx1 regulates development of neural-crest-derived branchial arch mesenchyme. *Development* **125**, 3005-3014.
Toledo, F., Liu, C. W., Lee, C. J. and Wahl, G. M. (2006). RMCE-ASAP: a gene targeting method for ES and somatic cells to accelerate phenotype analyses. *Nucleic Acids Res.* **34**, e92.
Trainor, P. A. and Tam, P. P. (1995). Cranial paraxial mesoderm and neural crest cells of the mouse embryo: co-distribution in the craniofacial mesenchyme but distinct segregation in branchial arches. *Development* **121**, 2569-2582.
Tucker, K. L., Wang, Y., Dausman, J. and Jaenisch, R. (1997). A transgenic mouse strain expressing four drug-selectable marker genes. *Nucleic Acids Res.* **25**, 3745-3746.
Wilkinson, D. (1992). *In Situ Hybridization: A Practical Approach*. Oxford: IRL Press.
Yamada, G., Mansouri, A., Torres, M., Stuart, E. T., Blum, M., Schultz, M., De Robertis, E. M. and Gruss, P. (1995). Targeted mutation of the murine goosecoid gene results in craniofacial defects and neonatal death. *Development* **121**, 2917-2922.
Yamauchi, Y., Abe, K., Mantani, A., Hitoshi, Y., Suzuki, M., Osuzu, F., Kuratani, S. and Yamamura, K. (1999). A novel transgenic technique that allows specific marking of the neural crest cell lineage in mice. *Dev. Biol.* **212**, 191-203.
Yanagisawa, H., Hammer, R. E., Richardson, J. A., Williams, S. C., Clouthier, D. E. and Yanagisawa, M. (1998). Role of endothelin-1/endothelin-A receptor-mediated signaling pathway in the aortic arch patterning in mice. *J. Clin. Invest.* **102**, 22-33.